OL | Organic Letters

Letter

Cite This: Org. Lett. XXXX, XXX, XXX−XXX

pubs.acs.org/OrgLett

Cucurbit[8]uril-Mediated Polypseudorotaxane for Enhanced Lanthanide Luminescence Behavior in Water

Weilei Zhou,[†,‡] Yong Chen,[†] Xianyin Dai,[†] Hao-yang Zhang,[†] and Yu Liu*[,†]

[†]College of Chemistry, State Key Laboratory of Elemento-Organic Chemistry, Nankai University, Tianjin 300071, P. R. China

[‡]Nano Innovation Institute (NII), College of Chemistry and Chemical Engineering, Inner Mongolia University for Nationalities, Tongliao 028000, People's Republic of China

Supporting Information

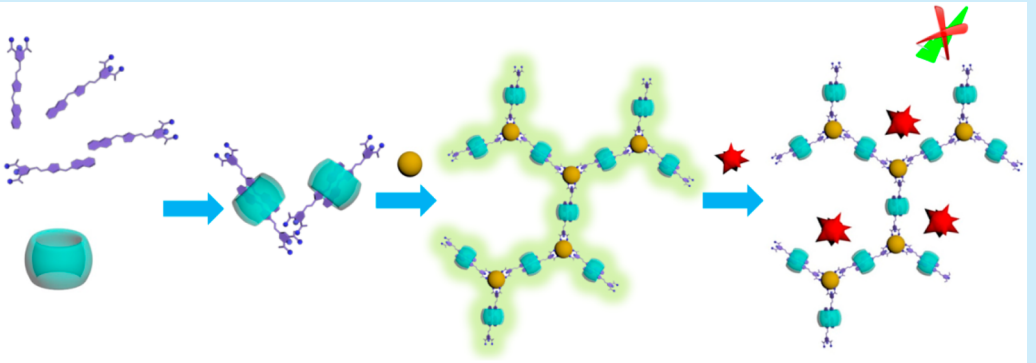

ABSTRACT: A novel supramolecular polypseudorotaxane was successfully constructed with pseudo[3]rotaxanes between pyridine-2,6-dicarboxylic acid imidazolium (G**1**) and cucurbit[8]uril (CB[8]) and the subsequent coordination with lanthanide ions. Significantly, compared with the pyridine-2,6-dicarboxylic acid imidazolium complex G**1**@Tb^{3+}, CB[8]-mediated polypseudorotaxane CB[8]@$G1_2$@Tb^{3+} not only displayed enhanced lanthanide luminescence behavior with a 29.1-fold time enhancement (from 45.76 μs to 1.33 ms) of the excited-state lifetime (τ) and a 8.7-fold increase (from 0.89% to 7.81%) in the quantum yield (Φ) but also exhibited a specific fluorescence response to antibiotics in an aqueous solution and a solid film.

Recently, much attention has been focused on interlocked molecules,[1] such as rotaxanes, catenanes, and knots,[2] due to their unique structures and properties.[3] Pseudorotaxanes or rotaxanes have been investigated most extensively as typical molecular machines, in which the inherent dynamic properties play an important role.[1b,4] The general protocols of constructing (pseudo)rotaxanes are created by one or more macrocycles and a linear guest as the wheel and the axle, respectively.[5] However, fluorescent rotaxanes are particularly rewarding because they are endowed with "bright" functions and applications[4,6] in areas such as nanotechnology,[7] smart materials,[6a,8] catalysts,[9] sensors,[6c,10] etc.

Cucurbit[*n*]urils (CB[*n*]) (*n* = 5−8, 10, and 14) make up a family of barrel-shaped macrocyclic molecular hosts that comprise different numbers of glycoluril units.[11] They have been utilized widely in the construction of various rotaxanes that benefit from their unique complexation behavior because the portal carbonyl groups of CB[*n*]s are favored to form complexes with the positively charged guests.[11a,c] In addition, the rotaxanes based on CB[*n*]s and fluorophore guest molecules could significantly promote the photophysical and photochemical properties of the guest fluorophore upon complexation.[11a,c,12] For example, Scherman et al.[13] reported a pseudorotaxane via the inclusion of CB[8] and perylene bis(diimide) dyes (PDI), and the fluorescence and the quantum yield were significantly enhanced because CB[8] effectively prevented the accumulation of PDI in an aqueous solution and the collision of other molecules with PDI. Park and co-workers[14] constructed a supramolecular polypseudorotaxane of CB[8] with cyanostilbene, where the weak fluorescence of cyanostilbene in aqueous solution (Φ < 1%) was greatly enhanced (Φ = 91%) upon formation of CB[8]-based polypseudorotaxane. Tao et al.[15] reported a white-light emissive polypseudorotaxane based on CB[8] and oligo(*p*-phenylenevinylene) in water by using different amounts of CB[8] in the supramolecular assembly. Recently, we also constructed a supramolecular assembly with near-infrared (NIR) emission by means of polypseudorotaxanes of an anthracene-based derivative and CB[8] with dodecyl-modified sulfonatocalix[4]arene, which was used in NIR lysosome-targeted cell imaging.[16]

On the other hand, among various metal−ligand complexes, Ln(III) complexes are particularly attractive for their unique luminescence properties, such as long-lived excited states, large Stokes shifts, visible-light emission, long luminescence life-

Received: October 11, 2019

DOI: 10.1021/acs.orglett.9b03597
Org. Lett. XXXX, XXX, XXX−XXX

times, and narrow emission bandwidths.[17] Nevertheless, most research involving lanthanide complexes (e.g., Eu^{3+} and Tb^{3+}) with chelate ligands was performed in aprotic organic solvents. Their emissions would be severely quenched by the O−H groups of the protic solvents (e.g., H_2O and CH_3OH), which greatly limited the applications.[18] Therefore, it is very important to design and synthesize lanthanide complexes with excellent luminescent properties in aqueous solution. Incorporation of a luminescent lanthanide into rotaxane may further tune the luminescent properties of the lanthanide. Herein, we utilized lanthanide coordination-driven self-assembly and CB[8]−imidazolium host−guest complexation to construct a supramolecular polypseudorotaxane that can have strong sensitizing ability with respect to not only Eu^{3+} but also Tb^{3+} in aqueous solution. First, pseudo[3]rotaxane was formed from the 1:2 inclusion complexation of CB[8] and pyridine-2,6-dicarboxylic acid imidazolium (G**1**) in aqueous solution through the host−guest interaction. Then, the coordination of the pseudo[3]rotaxane and lanthanide further led to the formation of polypseudorotaxane. More importantly, the resultant polypseudorotaxane CB[8]@G$\mathbf{1}_2$@Tb^{3+} exhibited a lifetime that was ≤29.1 times longer and a quantum yield that was ≤8.7 times higher than the corresponding values of G**1**@Tb^{3+}. Finally, the luminescent polypseudorotaxane CB[8]@G$\mathbf{1}_2$@Tb^{3+} exhibited good luminescence detectability for antibiotics in aqueous solution and the solid film.

The polypseudorotaxane was constructed from pseudo[3]-rotaxanes and lanthanide ions as shown in Scheme 1. The

Scheme 1. Schematic Illustration of Luminescent Lanthanide Supramolecular Polypseudorotaxane

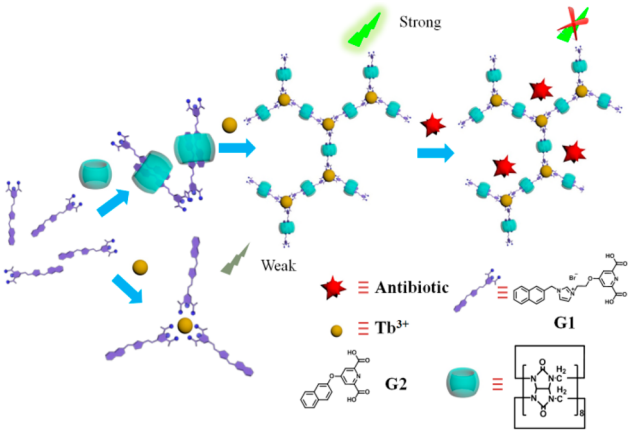

syntheses of compound G**1** and reference compound G**2** are shown in Figures S1−S6. Briefly, G**1** was prepared in 94% yield by the reaction of diethyl 4-(2-bromoethoxy)pyridine-2,6-dicarboxylate with 1-(naphthalen-2-ylmethyl)-1*H*-imidazole in CH_3CN and subsequent hydrolysis reaction.[19] It was well documented that CB[8] can accommodate two aryl-pyridinium molecules to form highly stable CB[8]-enhanced $\pi-\pi$ complexes.[12a,19] A similar phenomenon was observed in our system. The host−guest binding behaviors of CB[8] with G**1** were explored by ^1H NMR titration and isothermal titration calorimetry (ITC). In Figure S7, the titration of 0−0.5 equiv of CB[8] into the aqueous solution of G**1** indicated a 1:2 host−guest complexation. In the presence of CB[8], the proton signals of the naphthyl moiety in G**1** displayed an upfield shift and became clearly broadened, and the alkyl protons of the linker between naphthyl and pyridine-2,6-dicarboxylate groups exhibited a slight downfield shift. Meanwhile, when 0.5 equiv of CB[8] was gradually added, the methylene peak between the naphthalene group and the imidazole group at 5.49 ppm gradually disappeared, and a new peak at 5.43 ppm was generated due to the slow exchange equilibria. These experimental results revealed the CB[8]:G**1** stoichiometry was 1:2, and the naphthyl moiety of G**1** was inside the CB[8] as in the previous reports. Furthermore, ITC was used to measure the binding constants (K). As shown in Figure S8, the titration data could be fit well by using the "two successive binding sites" model of computer simulation. The K_{a1} and K_{a2} values between CB[8] and G**1** were calculated to be $(2.75 \pm 0.09) \times 10^6$ and $(1.08 \pm 0.6) \times 10^4$ M^{-1}, respectively. Upon the addition of CB[8] to the aqueous solution of G**1**, the UV−vis absorption band of naphthalene at 250−300 nm gradually decreased along with the appearance of two isosbestic points at 260 and 280 nm (Figure 1a), and the

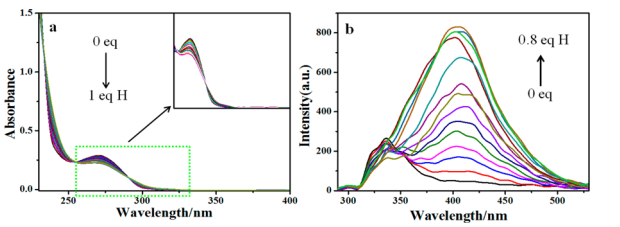

Figure 1. (a) Absorption spectra of G**1** (0.05 mM) with 1 equiv of CB[8]. (b) Emission spectra of G**1** (0.05 mM) with 0−0.8 equiv of CB[8] in water at 25 °C.

fluorescence emission of naphthalene at 335 nm decreased continuously, which was accompanied by an increase in the emission at 405 nm (Figure 1b). These phenomena jointly verified that two G**1** molecules were included in the CB[8] cavity to form a CB[8]@G$\mathbf{1}_2$ pseudo[3]rotaxane.

With the addition of the Tb^{3+} cation to the G**1** and CB[8]@G$\mathbf{1}_2$ pseudo[3]rotaxane solution, the absorption of G**1** and CB[8]@G$\mathbf{1}_2$ at 275 nm gradually increased, indicating the coordination of the Tb^{3+} cation with the carboxylic group of G**1** (Figure 2a and Figure S9). In addition, the emission spectra of either CB[8]@G$\mathbf{1}_2$@Tb^{3+} or G**1**@Tb^{3+} showed four sharp emission peaks at 490 nm ($^5D_4 \rightarrow {}^7F_6$), 545 nm ($^5D_4 \rightarrow {}^7F_5$), 583 nm ($^5D_4 \rightarrow {}^7F_4$), and 621 nm ($^5D_4 \rightarrow {}^7F_3$)[20a,c,21] (Figure 2b,c) assigned to the characteristic emission peak of Tb^{3+} via an energy transfer (ET) process from pyridine-2,6-dicarboxylate (DPA) to Tb^{3+}. The Tb^{3+}:G**1** coordination stoichiometry was investigated to be 1:3 through the fluorescence titration experiment by analyzing the curve of ΔF (complex-induced changes in fluorescence intensity at 545 nm) versus [Tb^{3+}]/[G**1**] molar ratio in panels c and d of Figure 2. This result was similar to the previous report that 3 equiv of pyridine-2,6-dicarboxylate (DPA) could strongly bind 1 equiv of lanthanide ions to form stable complexes.[20] Similarly, the Tb^{3+}:CB[8]@G$\mathbf{1}_2$ coordination stoichiometry was investigated to be 2:3.

In the fluorescence intensity measurement, the emission intensity at 545 nm of CB[8]@G$\mathbf{1}_2$@Tb^{3+} was 2 times higher than that of G**1**@Tb^{3+} at 8/15 equiv of Tb^{3+} (Figure 2b,c), indicating that the complexation of CB[8] could enhance the fluorescence of G**1**@Tb^{3+}. A similar enhancement of CB[8] toward the G**1**@Eu^{3+} complex was also observed (Figure S10). Significantly, the excited-state lifetime (τ = 1.33 ms) and

DOI: 10.1021/acs.orglett.9b03597
Org. Lett. XXXX, XXX, XXX−XXX

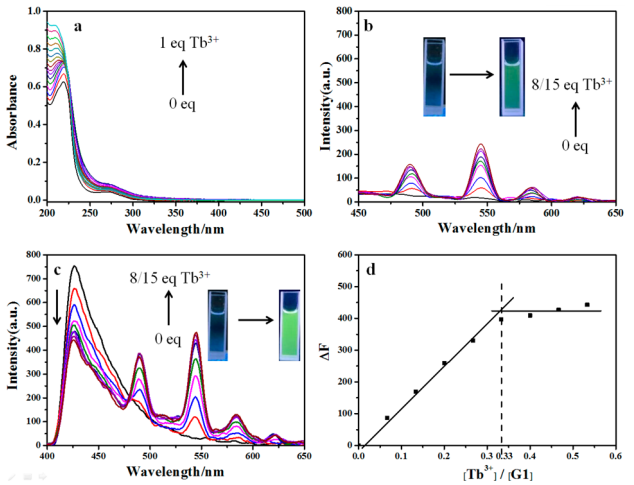

Figure 2. (a) Absorption spectra of CB[8]@G1$_2$ (0.01 mM) upon addition of 0−1 equiv of $Tb(NO_3)_3$ in H_2O (25 °C, pH 7.2). (b) Emission spectra of G1 (0.01 mM) with 8/15 equiv of Tb^{3+} in water (25 °C, pH 7.2). (c) Changes in emission of CB[8]@G1$_2$ (0.01 mM) upon addition of 0−8/15 equiv of $Tb(NO_3)_3$ in H_2O (25 °C, pH 7.2). (d) Change in emission intensity at 545 nm vs Tb^{3+}:G1 molar ratio. (λ_{ex} = 254 nm).

quantum yield (Φ = 7.81%) of CB[8]@G1$_2$@Tb^{3+} were 29.1 and 8.7 times higher, respectively, than the corresponding values of G1@Tb^{3+} [τ = 45.76 μs, and Φ = 0.89% (Figure 3

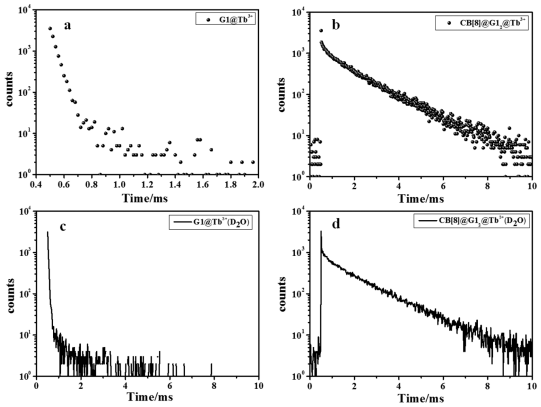

Figure 3. Fluorescence lifetimes of (a) G1@Tb^{3+}, (b) CB[8]@G1$_2$@Tb^{3+} in H_2O (25 °C, pH 7.2), (c) G1@Tb^{3+}, and (d) CB[8]@G1$_2$@Tb^{3+} in D_2O (25 °C, pH 7.2, 0.01 mM G1, λ_{ex} = 254 nm).

and Table 1)]. Similar enhancements of CB[8] toward the excited-state lifetime and quantum yield of the G1@Eu^{3+} complex were also observed (Figure S11 and Table 1).

Table 1. Luminescence Quantum Efficiencies (Φ), Lifetimes (τ), and Numbers of Water Molecules (q) Coordinated to Ln[a]

Sample	Φ (%)	τ_D	τ_H	q
G1@Tb^{3+}	0.89	46.73 μs	45.76 μs	1.96
CB[8]@G1$_2$@Tb^{3+}	7.81	1.48 ms	1.33 ms	0.10
G1@Eu^{3+}	2.74	–	1.22 ms	–
CB[8]@G1$_2$@Eu^{3+}	17.85	–	1.63 ms	–

[a] τ_D and τ_H represent the luminescence lifetimes determined in D_2O and H_2O, respectively.

Rationales for the significant enhancement of lifetime and quantum yield could be suggested. (1) The association of two G1 molecules in one CB[8] cavity led to the strong excimer emission. (2) The encapsulation of CB[8] toward G1 resulted in a more hydrophobic environment for the coordination Tb^{3+} center and reduced the coordination number of H_2O. (3) The strong interaction between CB[8] and G1 prevented the molecular rotation and reduced the energy loss of ligand molecules, leading to more energy matching. To verify this hypothesis, we estimated the number of water molecules for the coordination sphere of Ln^{3+} ions in G1@Tb^{3+} or CB[8]@G1$_2$@Tb^{3+} aqueous solution according to the reported method (see the Supporting Information).[20b] The luminescence lifetime of G1@Tb^{3+} was measured as 45.76 μs in H_2O and 46.73 μs in D_2O (Table 1). On the basis of these results, the coordinate number (q) of water molecules was 1.96 in the G1@Tb^{3+} aqueous solution, indicating approximately two water molecules were involved in the coordination of Tb^{3+}. In contrast, the luminescence lifetime of CB[8]@G1$_2$@Tb^{3+} increased to 1.33 ms in H_2O and 1.48 ms in D_2O. Therefore, the coordinate number (q) of water molecules decreased to 0.1 in the case of CB[8]@G1$_2$@Tb^{3+}, indicating that nearly no water molecule coordinated to Tb^{3+}. This efficient shielding of the luminescent Tb^{3+} center from the attack of water molecules consequently promotes the luminescence behavior of CB[8]@G1$_2$@Tb^{3+} to some extent. Meanwhile, a series of control experiments were carried out (Figures S12 and S13). First, we chose CB[5] that is not bound to G1 instead of CB[8]. With the addition of 1 equiv of CB[5] to G1@Tb^{3+}, the fluorescence of G1@Tb^{3+} did not change. Next, we also added 2 equiv of β-cyclodextrin, per-COOH-pillar[5]arene, and hepta-carboxyl-β-cyclodextrin to G1@Tb^{3+}, where β-cyclodextrin could bind the naphthalene moiety via a 1:1 stoichiometry, but per-COOH-pillar[5]arene or hepta-carboxyl-β-cyclodextrin interacted with only G1@Tb^{3+} via electrostatic attractions. The results showed that the luminescence of G1@Tb^{3+} was nearly unchanged or even weakened after the addition of these three macrocycles. On the other hand, we also used a neutral guest G2 as a reference compound. As compared with G1, G2 lacked the cationic imidazolium moiety and could not form the stable 2:1 complex with CB[8]. The results showed that the addition of CB[8] hardly affected the fluorescence of G2@Tb^{3+}. These jointly indicated that the increase in the fluorescence quantum yield and lifetime did not result from the coordination of cucurbituril with the lanthanide ions, and the 1:2 host−guest complexation between CB[8] and the naphthyl imidazolium moiety of G1 plays an important role. In addition to providing a more hydrophobic environment for the luminescent Tb^{3+} center, the strong association of CB[8] with G1 may restrict the rotation and thus reduce the energy loss of G1, which may also contribute to the enhanced luminescence property of CB[8]@G1$_2$@Tb^{3+}.

Furthermore, scanning electron microscopy (SEM) and transmission electron microscopy (TEM) were employed to investigate the morphology of G1, pseudo[3]rotaxanes CB[8]@G1$_2$, and polypseudorotaxane CB[8]@G1$_2$@Tb^{3+} (Figures S14 and S15). In SEM and TEM images, free G1 showed the morphology as needlelike nanofibers, but CB[8]@G1$_2$ showed the morphology as spheroidal nanoparticles. However, the morphology of CB[8]@G1$_2$@Tb^{3+} existed as rodlike blocks. Moreover, the ζ potentials of G1, G1@Tb^{3+}, CB[8]@G1$_2$, and CB[8]@G1$_2$@Tb^{3+} were measured to be −13.38, −2.58, −3.11, and 1.44 mV (Figure S16), respectively, indicating that

DOI: 10.1021/acs.orglett.9b03597
Org. Lett. XXXX, XXX, XXX−XXX

the surface electronegativity of G1 was increased through the inclusion of CB[8] and the coordination of Tb^{3+} with G1.

Because of the remarkably green luminescence and excellent water solubility, CB[8]@G$\mathbf{1}_2$@Tb^{3+} could be applied in detecting multiple antibiotics in water. As displayed in Figure S17 and Figure 4a, the different antibiotics (0.09 mM),

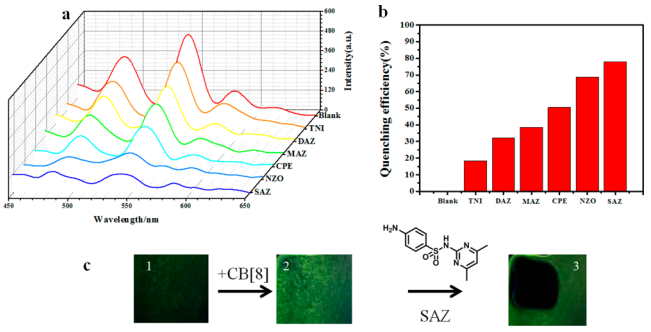

Figure 4. (a) Emission spectra of CB[8]@G$\mathbf{1}_2$@Tb^{3+} for different antibiotics in aqueous solution. (b) Corresponding luminescent quenching efficiency for the emission of the $^5D_4 \rightarrow {}^7F_5$ transition of CB[8]@G$\mathbf{1}_2$@Tb^{3+}. (c) Photographs of luminescent films of (1) G1@Tb^{3+}, (2) CB[8]@G$\mathbf{1}_2$@Tb^{3+}, and (3) CB[8]@G$\mathbf{1}_2$@Tb^{3+} in the presence of a SAZ aqueous solution (0.5 mM).

including nitrofurazone (NZO), metronidazole (MAZ), dimetridazole (DAZ), sulfamethazine (SAZ), chloramphenicol (CPE), and thiamphenicol (TNI), were added to the CB[8]@G$\mathbf{1}_2$@Tb^{3+} (0.01 mM G1) aqueous solution. Interestingly, CPE, NZO, or SAZ presented a decent quenching effect on polypseudorotaxane CB[8]@G$\mathbf{1}_2$@Tb^{3+}. The quenching efficiency was obtained by the ratio of the change in the luminescence intensity to the initial value $[(I_0 - I)/I_0]$ at the peak of 545 nm. SAZ and NZO gave a high (>70%) quenching efficiency; CPE gave a moderate (~51%) quenching efficiency, while the other three antibiotics gave weak (<40%) quenching efficiencies (Figure 4b), which may result from (1) electron transfer from CB[8]@G$\mathbf{1}_2$@Tb^{3+} in an excited state to the antibiotics[22] and (2) the competition of excitation energy coming from the strong absorption bands of CPE, NZO, and SAZ that significantly overlap with the absorption spectrum of CB[8]@G$\mathbf{1}_2$@Tb^{3+} as shown in Figure S18.[23] Then, we compared the fluorescence properties of G1@Tb^{3+} and CB[8]@G$\mathbf{1}_2$@Tb^{3+}doped in the solid PVA, and the polypseudorotaxane in Figure 4c shows a better luminescence effect. After that, we also tried to detect SAZ on the thin film. When 0.5 mM SAZ was dropped on the PVA, the green fluorescence completely disappears. These results clearly suggested that CB[8]@G$\mathbf{1}_2$@Tb^{3+} polypseudorotaxane can be used to selectively detect CPE, NZO, and SAZ in an aqueous solution and a solid film.

In conclusion, we successfully constructed a novel supramolecular polypseudorotaxane via the coordination of pseudo[3]rotaxanes with lanthanide ions. Such pseudo[3]rotaxanes were formed by the 2:1 complexation stoichiometry between G1 and CB[8]. Significantly, polypseudorotaxane CB[8]@G$\mathbf{1}_2$@Tb^{3+} not only increased the lifetime from 45.76 μs to 1.33 ms (29.1-fold) but also enhanced the quantum yield from 0.89% to 7.81% (8.7-fold) as compared with G1@Tb^{3+}. Significantly, the polypseudorotaxane constructed by coordination of pseudo[3]rotaxanes with Tb^{3+} could detect SAZ, NZO, and CPE in an aqueous solution and a solid film. We believe this could provide a new design idea for the application of luminescent lanthanide complexes in the detection of antibiotics in water.

■ ASSOCIATED CONTENT

Supporting Information

The Supporting Information is available free of charge on the ACS Publications website at DOI: 10.1021/acs.orglett.9b03597.

Experimental section, Figures S1−S19, and additional references (PDF)

■ AUTHOR INFORMATION

Corresponding Author

*E-mail: yuliu@nankai.edu.cn.

ORCID

Yu Liu: 0000-0001-8723-1896

Notes

The authors declare no competing financial interest.

■ ACKNOWLEDGMENTS

The authors thank the NNSFC (21672113, 21772099, 21861132001, and 21971127) for financial support.

■ REFERENCES

(1) (a) Lewis, J. E. M.; Beer, P. D.; Loeb, S. J.; Goldup, S. M. *Chem. Soc. Rev.* **2017**, *46*, 2577−2591. (b) Sluysmans, D.; Stoddart, J. F. *Trends in Chemistry* **2019**, *1*, 185−197.

(2) (a) Jamieson, E. M. G.; Modicom, F.; Goldup, S. M. *Chem. Soc. Rev.* **2018**, *47*, 5266−5311. (b) Ji, X.; Chi, X.; Ahmed, M.; Long, L.; Sessler, J. L. *Acc. Chem. Res.* **2019**, *52*, 1915−1927. (c) Mohankumar, M.; Holler, M.; Meichsner, E.; Nierengarten, J. F.; Niess, F.; Sauvage, J. P.; Delavaux-Nicot, B.; Leoni, E.; Monti, F.; Malicka, J. M.; Cocchi, M.; Bandini, E.; Armaroli, N. *J. Am. Chem. Soc.* **2018**, *140*, 2336−2347. (d) Zhong, J.; Zhang, L.; August, D.; Whitehead, G. F. S.; Leigh, D. A. *J. Am. Chem. Soc.* **2019**, *141*, 14249−14256.

(3) (a) Leung, F. K. C.; Kajitani, T.; Stuart, M. C. A.; Fukushima, T.; Feringa, B. L. *Angew. Chem., Int. Ed.* **2019**, *58*, 10985−10989. (b) Cai, K.; Lipke, M. C.; Liu, Z.; Nelson, J.; Cheng, T.; Shi, Y.; Cheng, C.; Shen, D.; Han, J. M.; Vemuri, S.; Feng, Y.; Stern, C. L.; Goddard, W. A.; Wasielewski, M. R.; Stoddart, J. F. *Nat. Commun.* **2018**, *9*, 5275.

(4) (a) Ma, X.; Tian, H. *Chem. Soc. Rev.* **2010**, *39*, 70−80. (b) Cui, Y. − H.; Deng, R.; Li, Z.; Du, X.−S.; Jia, Q.; Wang, X.−H.; Wang, C.−Y.; Meguellati, K.; Yang, Y.−W. *Mater. Chem. Front.* **2019**, *3*, 1427−1432. (c) Zhou, W.; Zhao, X.; Chen, Y.; Liu, Y. *Org. Chem. Front.* **2019**, *6*, 10−14. (d) Wang, K.; Cai, X.; Yao, W.; Tang, D.; Kataria, R.; Ashbaugh, H. S.; Byers, L. D.; Gibb, B. C. *J. Am. Chem. Soc.* **2019**, *141*, 6740−6747. (e) Zhang, Y.; Chen, Y.; Li, J.−J.; Liang, L.; Liu, Y. *Huaxue Xuebao* **2018**, *76*, 622−626.

(5) (a) Yamaguchi, N.; Hamilton, L. M.; Gibson, H. W. *Angew. Chem., Int. Ed.* **1998**, *37*, 3275−3279. (b) Fielden, S. D. P.; Leigh, D. A.; McTernan, C. T.; Perez-Saavedra, B.; Vitorica-Yrezabal, I. J. *J. Am. Chem. Soc.* **2018**, *140*, 6049−6052.

(6) (a) Ma, X.; Zhang, J.; Cao, J.; Yao, X.; Cao, T.; Gong, Y.; Zhao, C.; Tian, H. *Chem. Sci.* **2016**, *7*, 4582−4588. (b) Tian, H.; Wang, Q. C. *Chem. Soc. Rev.* **2006**, *35*, 361−374. (c) Yu, X.; Liang, W.; Huang, Q.; Wu, W.; Chruma, J. J.; Yang, C. *Chem. Commun.* **2019**, *55*, 3156−3159.

(7) (a) Kay, E. R.; Leigh, D. A. *Angew. Chem., Int. Ed.* **2015**, *54*, 10080−10088. (b) Barrell, M. J.; Campana, A. G.; von Delius, M.; Geertsema, E. M.; Leigh, D. A. *Angew. Chem., Int. Ed.* **2011**, *50*, 285−290. (c) Kassem, S.; van Leeuwen, T.; Lubbe, A. S.; Wilson, M. R.; Feringa, B. L.; Leigh, D. A. *Chem. Soc. Rev.* **2017**, *46*, 2592−2621. (d) Panman, M. R.; van Dijk, C. N.; Huerta-Viga, A.; Sanders, H. J.;

DOI: 10.1021/acs.orglett.9b03597
Org. Lett. XXXX, XXX, XXX−XXX

Bakker, B. H.; Leigh, D. A.; Brouwer, A. M.; Buma, W. J.; Woutersen, S. *Nat. Commun.* **2017**, *8*, 2206.
(8) (a) Cheng, S. C.; Chen, K. J.; Suzaki, Y.; Tsuchido, Y.; Kuo, T. S.; Osakada, K.; Horie, M. *J. Am. Chem. Soc.* **2018**, *140*, 90−93. (b) Wu, H.; Chen, Y.; Dai, X.; Li, P.; Stoddart, J. F.; Liu, Y. *J. Am. Chem. Soc.* **2019**, *141*, 6583−6591. (c) Wang, S.; Xu, Z.; Wang, T.; Xiao, T.; Hu, X.−Y.; Shen, Y.−Z.; Wang, L. *Nat. Commun.* **2018**, *9*, 1737. (d) Samanta, S. K.; Quigley, J.; Vinciguerra, B.; Briken, V.; Isaacs, L. *J. Am. Chem. Soc.* **2017**, *139*, 9066−9074.
(9) (a) Blanco, V.; Leigh, D. A.; Marcos, V. *Chem. Soc. Rev.* **2015**, *44*, 5341−5370. (b) Leigh, D. A.; Marcos, V.; Wilson, M. R. *ACS Catal.* **2014**, *4*, 4490−4497.
(10) (a) Denis, M.; Qin, L.; Turner, P.; Jolliffe, K. A.; Goldup, S. M. *Angew. Chem., Int. Ed.* **2018**, *57*, 5315−5319. (b) Denis, M.; Goldup, S. M. *Angew. Chem., Int. Ed.* **2018**, *57*, 4462−4464. (c) Denis, M.; Pancholi, J.; Jobe, K.; Watkinson, M.; Goldup, S. M. *Angew. Chem., Int. Ed.* **2018**, *57*, 5310−5314.
(11) (a) Barrow, S. J.; Kasera, S.; Rowland, M. J.; del Barrio, J.; Scherman, O. A. *Chem. Rev.* **2015**, *115*, 12320−12406. (b) Gao, C.; Huang, Q.; Lan, Q.; Feng, Y.; Tang, F.; Hoi, M. P. M.; Zhang, J.; Lee, S. M. Y.; Wang, R. *Nat. Commun.* **2018**, *9*, 2967. (c) Yu, G.; Jie, K.; Huang, F. *Chem. Rev.* **2015**, *115*, 7240−7303.
(12) (a) Jiao, D. Z.; Biedermann, F.; Tian, F.; Scherman, O. A. *J. Am. Chem. Soc.* **2010**, *132*, 15734−15743. (b) Zhao, X.; Liu, F.; Zhao, Z.; Karoui, H.; Bardelang, D.; Ouari, O.; Liu, S. *Org. Biomol. Chem.* **2018**, *16*, 3809−3815.
(13) Biedermann, F.; Elmalem, E.; Ghosh, I.; Nau, W. M.; Scherman, O. A. *Angew. Chem., Int. Ed.* **2012**, *51*, 7739−7743.
(14) Kim, H. J.; Whang, D. R.; Gierschner, J.; Park, S. Y. *Angew. Chem., Int. Ed.* **2016**, *55*, 15915−15919.
(15) Ni, X. L.; Chen, S.; Yang, Y.; Tao, Z. *J. Am. Chem. Soc.* **2016**, *138*, 6177−6183.
(16) Chen, X. M.; Chen, Y.; Yu, Q.; Gu, B. H.; Liu, Y. *Angew. Chem., Int. Ed.* **2018**, *57*, 12519−12523.
(17) (a) Muller, G. *Dalton Trans* **2009**, 9692−9707. (b) Bunzli, J−G. G.; Piguet, C. *Chem. Rev.* **2002**, *102*, 1897−1928. (c) Heine, J.; Muller-Buschbaum, K. *Chem. Soc. Rev.* **2013**, *42*, 9232−9242.
(18) (a) Kai, T.; Kishimoto, M.; Akita, M.; Yoshizawa, M. *Chem. Commun.* **2018**, *54*, 956−959. (b) Weng, G.; Thanneeru, S.; He, J. *Adv. Mater.* **2018**, *30*, 1706526.
(19) Zhang, W.; Zhang, H. Y.; Zhang, Y. H.; Liu, Y. *Chem. Commun.* **2015**, *51*, 16127−16130.
(20) (a) Han, M.; Zhang, H. Y.; Yang, L. X.; Jiang, Q.; Liu, Y. *Org. Lett.* **2008**, *10*, 5557−5560. (b) Li, B.; Ding, Z.−J.; Li, Z.; Li, H. *J. Mater. Chem. C* **2018**, *6*, 6869−6874. (c) Zhou, W. L.; Chen, Y.; Yu, Q.; Li, P.; Chen, X.; Liu, Y. *Chem. Sci.* **2019**, *10*, 3346−3352.
(21) (a) Zhou, Y.; Zhang, H. Y.; Zhang, Z. Y.; Liu, Y. *J. Am. Chem. Soc.* **2017**, *139*, 7168−7171. (b) Zhou, Y.; Zhang, H. Y.; Liu, Y. *J. Photochem. Photobiol., A* **2018**, *355*, 242−248.
(22) (a) Zhu, X.−D.; Zhang, K.; Wang, Y.; Long, W.−W.; Sa, R.−J.; Liu, T.−F.; Lu, J. *Inorg. Chem.* **2018**, *57*, 1060−1065. (b) Wen, L.; Zheng, X.; Lv, K.; Wang, C.; Xu, X. *Inorg. Chem.* **2015**, *54*, 7133−7135. (c) Malik, A. H.; Iyer, P. K. *ACS Appl. Mater. Interfaces* **2017**, *9*, 4433−4439.
(23) (a) Zhu, Q.−Q.; He, H.; Yan, Y.; Yuan, J.; Lu, D.−Q.; Zhang, D.−Y.; Sun, F.; Zhu, G. *Inorg. Chem.* **2019**, *58*, 7746−7753. (b) Dong, B.−X.; Pan, Y.−M.; Liu, W.−L.; Teng, Y.−L. *Cryst. Growth Des.* **2018**, *18*, 431−440. (c) He, H.; Zhu, Q.−Q.; Li, C.−P.; Du, M. *Cryst. Growth Des.* **2019**, *19*, 694−703.

DOI: 10.1021/acs.orglett.9b03597
Org. Lett. XXXX, XXX, XXX−XXX